Contents lists available at ScienceDirect

Sensors and Actuators B: Chemical

Intensity modulated refractive index sensor based on optical fiber Michelson interferometer

Jiangtao Zhou, Yiping Wang*, Changrui Liao, Bing Sun, Jun He, Guolu Yin, Shen Liu, Zhengyong Li, Guanjun Wang, Xiaoyong Zhong, Jing Zhao

Key Laboratory of Optoelectronic Devices and Systems of Ministry of Education and Guangdong Province, College of Optoelectronic Engineering, Shenzhen University, Shenzhen 518060, China

ARTICLE INFO

ABSTRACT

We demonstrated a refractive index (RI) sensor based on optical fiber Michelson interferometer (MI), which was fabricated by splicing a section of thin core fiber (TCF) to a standard single mode fiber with a core offset. Experimentally, such a MI-based RI sensor with a core offset of 8 μm and a TCF length of 3 mm exhibits a high resolution of 4.9×10^{-6} RIU and sensitivity of −202.46 dB/RIU, which is two or three times higher than that of intensity-modulated RI sensors reported previously. In contrast, our MI-based RI sensor is insensitive to temperature, thus overcoming the cross-sensitivity problem between surrounding RI and temperature. Moreover, intensity modulation, rather than wavelength modulation, was used in the proposed MI-based RI sensor, and the sensor also has the advantages of compact size (8 mm), simple structure, easy fabrication, and good repeatability.

© 2014 Published by Elsevier B.V.

1. Introduction

Over the past decades, various refractive index (RI) sensors, e.g. Abbe refractometer, have been demonstrated for different applications. But traditional refractometers have the disadvantages of big size and weight. In recent years, optical fiber RI sensors were widely employed in the field of chemical and biochemical sensing applications because of their attractive characteristics, such as remote sensing, immunity to electromagnetic interference, corrosion resistance, small size, high sensitivity, and ultra-fast response [1]. A few types of optical fiber RI sensors have accordingly been demonstrated by means of employing fiber Bragg gratings (FBGs) [2], long period fiber gratings (LPFGs) [3–5], Mach–Zender interferometers (MZIs) [6], surface plasmon resonance (SPR) [7,8], Fabry–Perot interferometers (FPIs) [9,10], Michelson interferometers (MIs) [11–13], and photonic crystal fibers (PCFs) [14]. However, these approaches have their respective drawbacks. For example, LPFG and FBG-based sensors exhibited the cross-sensitivity between refractive index and temperature [15]. FPIs-based sensor exhibited a low sensitivity in the RI sensing applications [16]. PCFs required relatively expensive structures and complex fabrication process [14]. In addition, MI-based sensors usually utilize the

wavelength modulation, rather than intensity-modulation, for RI measurement, which requires complex and expensive wavelength de-modulation devices [12,13].

In this paper, we demonstrated a high-sensitive intensity-modulated refractive index sensor based on an in-fiber Michelson interferometer which was fabricated by means of splicing a section of thin core fiber (TCF) to a standard single-mode fiber (SMF) with a lateral offset. The lateral offset and the TCF length were optimized to enhance the fringe contrast of the MI. Several advantages are involved in the proposed sensor, such as a short size and a simple structure, a high sensitivity of −202.46 dB/RIU, and insensitivity to temperature.

2. Sensor fabrication

As shown in Fig. 1(a), a broad band source (BBS) with a laser wavelength range from 1250 to 1650 nm, an optical spectrum analyzer (OSA) (ANDO AQ6317B) and an optical circulator were employed to monitor the reflection spectrum of the proposed MI-based sensor, which was fabricated as described below. Firstly, a section of TCF (Nufern UHNA-3) with core and cladding diameters of 4 and 125 μm, respectively, was spliced to a standard SMF, i.e. Lead-in SMF, with a 6 μm lateral offset between the two fiber cores by use of a commercial fusion splicer machine (Fujikura, FSM-100P+), in which there are two pairs of motors, i.e. the axial and vertical moving motors, with a movement accuracy of 0.01 and
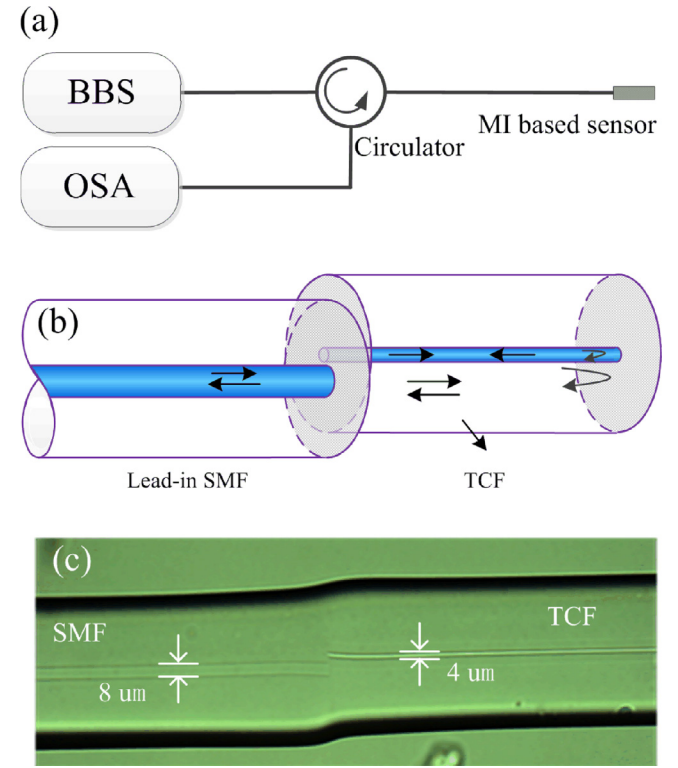
Fig. 1. (a) Schematic diagram of the proposed MI-based sensor system; (b) schematic diagram and (c) microscope image of the MI-based sensor.

misalignment-spliced joint, resulting in Michelson interference in the core of the SMF. Thus, a MI-based sensor was achieved, and visible interference fringe pattern were observed in the reflection spectrum, as shown in Fig. 2(a). According to Michelson interference, the fringe contrast in the interference pattern depends strongly on the ratio of lights coupled into the core and cladding modes in the TCF and their transmission loss, so it is essential to improve the TCF length and the core offset for enhancing the interference fringe contrast.

Thus the TCF was repeatedly cleaved to gradually shorten the TCF to a desired length by employing a microscope-assisted cleaving technique, accordingly achieving seven MI samples with a core offset 6 μm and different TCF lengths of 20, 10, 8, 5, 3, 1.5 and 0.5 mm. Fig. 2(a) illustrates four of the seven MI interference patterns. Each MI sample with different TCF length exhibits distinct fringe contrast in the interference patterns, as shown in Fig. 2(a). And it can be found in the insert of Fig. 2(a) that the MI sample with a TCF length of 3 mm has the largest fringe contrast of 12.56 dB. Moreover, we calculated the free spectrum range (FSR) of the interference fringes by

$$\Delta\lambda_{dip}^m \approx \frac{\lambda^2}{2\Delta n_{eff}^m L} \tag{1}$$

Δn_{eff}^m is the effective RI difference between the core and mth cladding modes in the TCF, L is the length of the TCF. As shown in Fig. 2(b), the measured FSR of the seven MI samples is 1.1, 2.4, 3.3, 4.4, 6.6, 19.2 and 49.7 nm, respectively, which shows a good agreement with the calculated value.

Furthermore, the core offset between the SMF and the TCF was improved to enhance the fringe contrast in the interference pattern by moving the X- and Y-directional motors in the splicer. Another six MI samples with a TCF length of 3 mm and different core offsets of 2, 4, 6, 8, 10, and 12 μm, respectively, were fabricated. Fig. 3 illustrates four of the six MI interference patterns. As shown in Fig. 3, each MI sample with a certain core offset exhibits distinct fringe contrast in the interference patterns due to the core-offset-induced change of the ratio of lights coupled into the core and cladding modes in the TCF. And it can be found in the insert of Fig. 3 that the MI sample with a core offset of 8 μm and a TCF length of 3 mm has the largest fringe contrast of 18.21 dB.
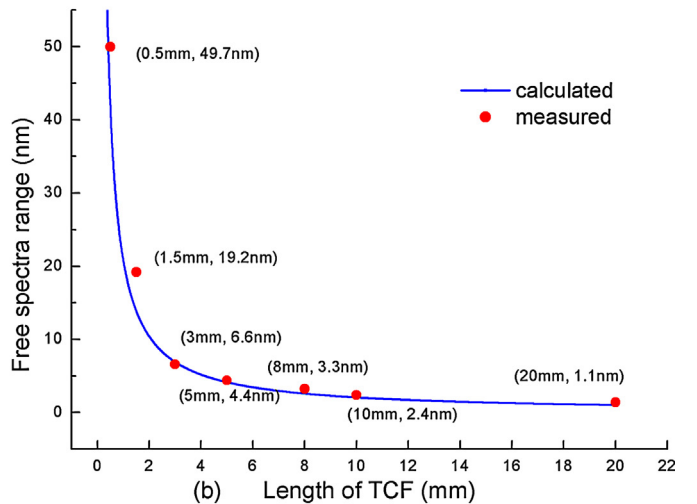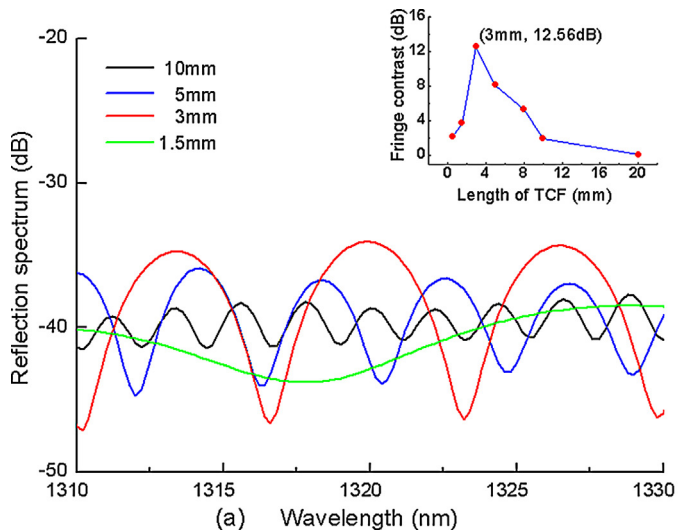
0.1 μm, respectively. Then, another end of the TCF was cleaved with a length of 20 mm. Consequently, as shown in Fig. 2(a), a clear interference fringes pattern was observed in the reflection spectrum.

As shown in Fig. 1(b), light transmitting in the SMF is divided into two parts at the misalignment-spliced joint. A part of light is coupled into the core of the TCF as a core mode, and another part of light is coupled into the cladding of the TCF as cladding modes. The two part of light will be reflected at the cleaved ends of the PCF and then re-coupled into the core of the lead-in SMF at the

Fig. 2. (a) Reflection spectra of the four MI samples with a core offset of 6 μm and TCF lengths of 1.5, 3, 5, and 10 mm, respectively; the insert shows the fringe contrasts in the interference patterns of the seven MI samples as a function of the measured TCF length; (b) measured and calculated FSR of the interference fringes of the MI sensor samples with different TCF lengths.
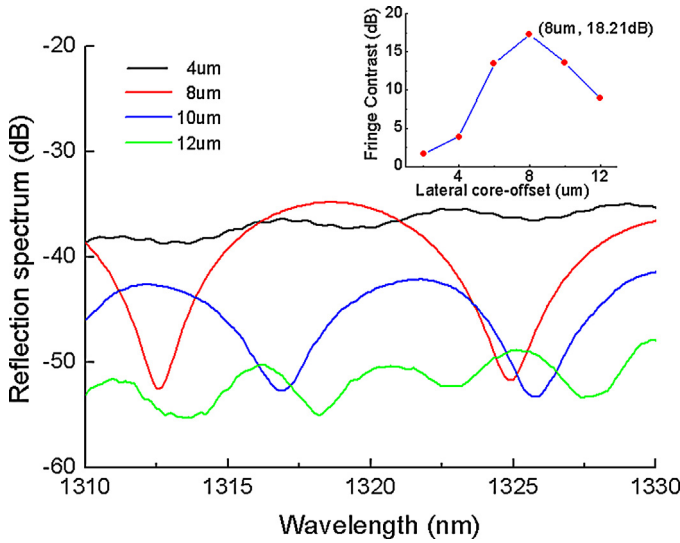
Fig. 3. Reflection spectra of the MI-based samples with a TCF length of 3 mm and core-offsets of 4, 8, 10, 12 μm, respectively; the insert shows the fringe contrast in the interference patterns of the six MI samples with different core offsets.

3. Application and discussion

Due to the fact that the interference pattern is mainly formed by the core and cladding modes, the intensity of the interference pattern can be calculated as [13,17]:

$$I = \left(I_{\text{core}} + \sum_m I_{\text{clad}}^m + \sum_m 2\sqrt{I_{\text{core}} \cdot I_{\text{clad}}^m} \cdot \text{Cos}\, \Phi^m \right) \cdot R \qquad (2)$$

where I_{core} and I_{clad}^m are the light intensity of the core mode, and the mth cladding mode, respectively; Φ^m is the phase delay between the core mode and the mth cladding mode. R is the reflectivity on the cleaved endface of the TCF and can be given by [18,19]:

$$R = \frac{(n_{\text{core}} - n)^2}{(n_{\text{core}} + n)^2} \qquad (3)$$

where n_{core} and n are the RI of the fiber core and surrounding medium, respectively. According to Eqs. (2) and (3), the intensity of the interference pattern depends strongly on the surrounding RI.

Hence, our misalignment-spliced MI-based structure could be used to develop a promising RI sensor. Accordingly, another misalignment-spliced MI sample with optimized parameters, i.e. a core offset of 8 μm and a TCF length of 3 mm was fabricated to investigate its response to surrounding RI and temperature. As shown in Fig. 4, the interference pattern of the proposed MI-based sensor exhibits a large fringe contrast of up to 18.85 dB. The insertion loss of our MI-based RI sensor was measured to be about −34 dB, which is approximate to those (about −42 dB [20] and about −32 dB [21]) of other RI sensing devices based on Fresnel reflection [20] and multimode interference [21].

3.1. Response to refractive index

The MI-based sensor illustrated in Fig. 4 was orderly immersed into a series of commercial refractive index matching liquids (Cargille Lab, http://www.cargille.com) with a RI from 1.30 to 1.43 with a step of 0.01 to investigate its response to surrounding RI. After each investigation, the MI-based sensor was dipped into alcohol for 5 min in order to remove the matching liquid adhered on the fiber surface. In order to avoid the disturbance of the liquid pressure, each RI measurement was performed at the same liquid
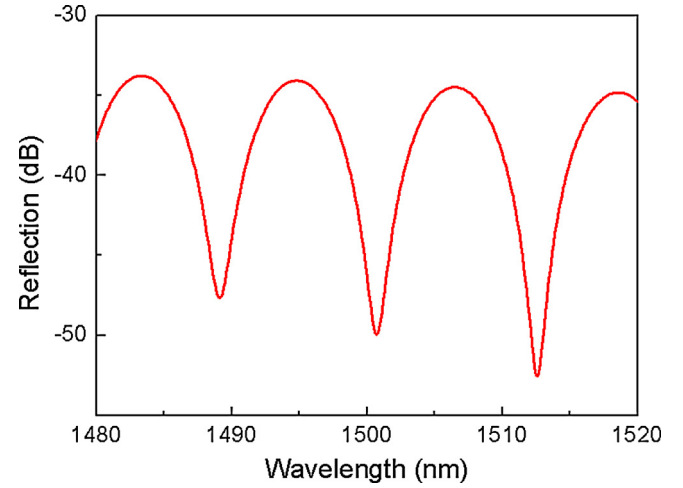

Fig. 4. Reflection spectrum of the proposed MI-based sensor with a core offset of 8 μm and a TCF length of 3 mm.

level. As shown in Fig. 5(a), while the surrounding RI increased, the reflection spectrum of the MI-based sensor shifted toward a shorter wavelength and the light intensity decreased gradually. As shown in Fig. 5(b), the changes of the fringe dip wavelength and intensity with surrounding RI show good agreements with the polynomial fitting curves.

As shown in Fig. 5(b), the RI sensitivity of the MI-based sensor was calculated to be −202.46 dB/RIU at the refractive index of 1.42 via polynomial fitting method, which is two or three times larger than those (27 dB/RIU [16], 94.58 dB/RIU [20], and −110 dB/RIU [21]) of the intensity-modulated RI sensors reported previously. Moreover, the intensity modulation, rather than the wavelength modulation [22], was used in our proposed MI-based RI sensor, which solves the cross-sensitivity problem between temperature and surrounding RI, as described below.

3.2. Response to temperature

The proposed MI-based sensor was placed in a tube furnace with a temperature range from room temperature to 100 °C in order to investigate its temperature response. Temperature in the furnace rose gradually from 30 °C to 100 °C with a step of 10 °C and maintained about 30 min after each temperature heating. As shown in Fig. 6(a), while temperature rose, the dip wavelength of interference fringe shifted linearly toward a longer wavelength with a sensitivity of 42 pm/°C, in contrast, the dip intensity of interference fringe hardly changed. Temperature-induced 'red' shift of the dip wavelength could be explained below: since thermo-optic coefficient of the Ge-doped silica core is higher than that of the cladding consisting of fused silica, effective refractive index difference between the core and the cladding modes will increase with temperature rise [23,24]. As a result, the dip wavelength shifts toward a longer wavelength due to the temperature-induced change of effective index difference while surrounding temperature rises. As shown in Fig. 6(b), the dip intensity hardly changed while temperature rose, and the maximum temperature-induced intensity change is ±0.028 dB. Thus the temperature-induced RI measurement error is less than $\pm 1.38 \times 10^{-4}$ without using temperature compensation, which is similar to that ($\pm 5 \times 10^{-4}$) of the RI sensor reported in Ref. [25].

4. Discussion

As shown in Figs. 5(b) and 6(b), the dip intensity of interference fringes decreases with the increase of surrounding RI, whereas
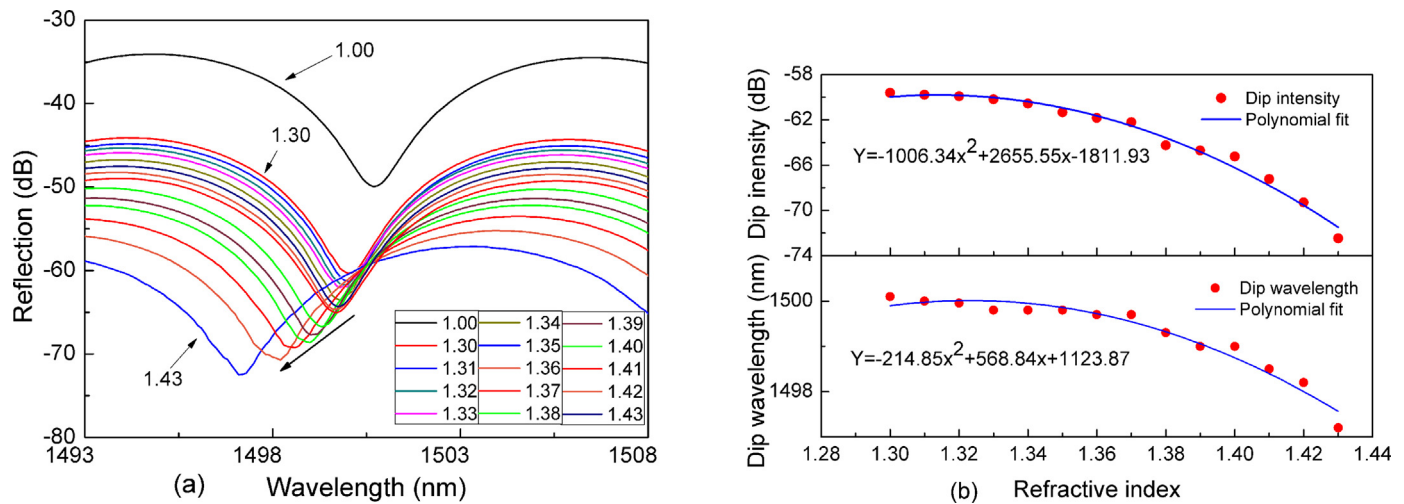
Fig. 5. (a) Reflection spectra evolution of the MI-based sensor with different surrounding RI from 1.30 to 1.43; (b) measured fringe dip intensity (upper) and wavelength (lower) versus surrounding RI and their polynomial fits.
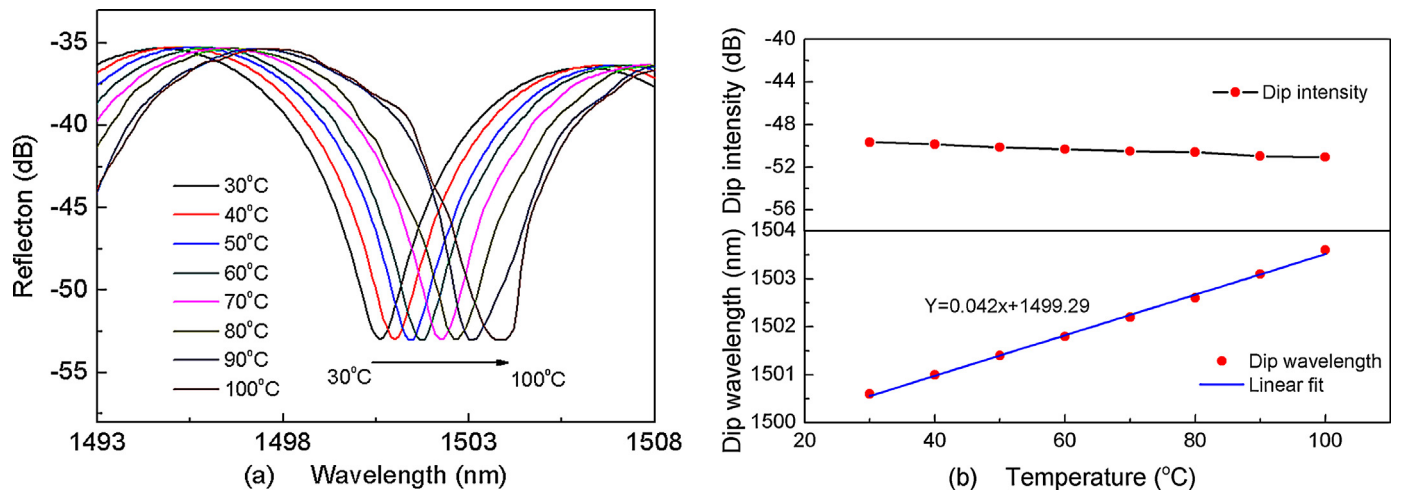

Fig. 6. (a) Reflection spectrum evolution of the MI-based sensor with different temperatures; (b) measured fringe dip intensity (upper) and wavelength (lower) versus temperature and their linear fits.

it is insensitive to temperature. Hence, the misalignment-spliced MI could be used to develop a promising intensity-modulated RI sensor with temperature insensitivity, which overcomes the cross-sensitivity between surrounding RI and temperature in the practical sensing applications. The proposed MI-based RI sensor exhibits a high sensitivity of −202.46 dB/RIU at the refractive index of 1.42. The resolution of our proposed RI sensor depends on the resolution of the instrument employed to measure the intensity of the output light. Provided that an optical spectrum analyzer with a resolution of 0.001 dB is employed to measure the output power of our proposed RI sensor, a high RI resolution of 4.9×10^{-6} RIU could be achieved, which is about one order higher than that (4.2×10^{-5} RIU [16] and 3.8×10^{-5} RIU [21]) of the RI sensor reported in Refs. [16,21].

The reason why we choose the TCF (Nufern UHNA-3) is that it exhibits a high number aperture (NA) of 0.35, which lead to an ability of gathering more light into the core rather than the loss from the fiber cladding. Our experiments showed that this type of TCF cannot be replaced with a low NA fiber, e.g. SMF-28. To verify the repeatability of our fabrication process, additional several MI-based samples with the optimized parameters had been fabricated and a good repeatability of the interference spectra was achieved. Moreover, our MI-based sensor with improved parameters (8 μm

core offset and 3 mm TCF length) exhibits a larger fringe contrast of up to 18 dB than other MI-based devices [13,20].

5. Conclusion

A novel and compact fiber MI-based sensor was demonstrated by means of splicing a section of TCF to a standard SMF with a core offset. The core offset and the TCF length were improved to 8 μm and 3 mm, respectively, in order to achieve a large fringe contrast of up to 18 dB. Such a MI-based RI sensor based on intensity modulation exhibits a high sensitivity of at the −202.46 dB/RIU at the refractive index of 1.42, which is two or three times higher than that of other intensity-modulated RI sensors reported previously. Moreover, the RI sensor is insensitive to temperature, thus overcoming the cross sensitivity problem between surrounding RI and temperature. Our MI-based RI sensor also exhibits the advantages of compact size (8 mm), simple structure, easy fabrication, and good repeatability. However, a complex and large spectrum analyzer has to be employed to measure the change of the dip intensity in our current experiments, which is disadvantageous to RI measurements. So in the practical sensing applications, a simple

demodulation device should be developed to measure the intensity at the dip wavelength.

Acknowledgements

References

[1] N.S. Kapany, J.N. Pike, Fiber optics. Part IV. A photorefractometer, J. Opt. Soc. Am. 47 (1957) 1109–1114.
[2] A. Iadicicco, S. Campopiano, A. Cutolo, M. Giordano, A. Cusano, Self temperature referenced refractive index sensor by non-uniform thinned fiber Bragg gratings, Sens. Actuators B: Chem. 120 (2006) 231–237.
[3] Y. Tan, W. Ji, V. Mamidala, K. Chow, S. Tjin, Carbon-nanotube-deposited long period fiber grating for continuous refractive index sensor applications, Sens. Actuators B: Chem. 196 (2014) 260–264.
[4] T. Zhu, Y.J. Rao, Q.J. Mo, Simultaneous measurement of refractive index and temperature using a single ultra-long-period fiber grating, IEEE Photon. Technol. Lett. 17 (2005) 2700–2702.
[5] Y. Wang, L. Xiao, D.N. Wang, W. Jin, Highly sensitive long-period fiber-grating strain sensor with low temperature sensitivity, Opt. Lett. 31 (2006) 3414–3416.
[6] R. Bernini, A. Cusano, Generalized Mach–Zehnder interferometers for sensing applications, Sens. Actuators B: Chem. 100 (2004) 72–74.
[7] H. Liang, H. Miranto, N. Granqvist, J.W. Sadowski, T. Viitala, B. Wang, M. Yliperttula, Surface plasmon resonance instrument as a refractometer for liquids and ultrathin films, Sens. Actuators B: Chem. 149 (2010) 212–220.
[8] J.L. Qu, L.X. Liu, Y.H. Shao, H.B. Niu, B. Gao, Recent progress in multifocal multi-photon microscopy, J. Innov. Opt. Health Sci. 5 (3) (2012) 1250018–1250021.
[9] Y. Wang, D. Wang, C. Liao, T. Hu, J. Guo, H. Wei, Temperature-insensitive refractive index sensing by use of micro Fabry–Pérot cavity based on simplified hollow-core photonic crystal fiber, Opt. Lett. 38 (2013) 269–271.
[10] C. Liao, T. Hu, D. Wang, Optical fiber Fabry–Perot interferometer cavity fabricated by femtosecond laser micromachining and fusion splicing for refractive index sensing, Opt. Express 20 (2012) 22813–22818.
[11] Z. Li, Y. Wang, C. Liao, S. Liu, J. Zhou, X. Zhong, Y. liu, K. Yang, Q. Wang, G. Yin, Temperature-insensitive refractive index sensor based on in-fiber Michelson interferometer, Sens. Actuators B: Chem. 199 (2014) 31–35.
[12] Y. Wang, J. Chen, X. Li, X. Zhang, J. Hong, A. Ye, Simultaneous measurement of various optical parameters in a multilayer optical waveguide by a Michelson precision reflectometer, Opt. Lett. 30 (2005) 979–981.
[13] Q. Rong, X. Qiao, Y. Du, D. Feng, R. Wang, Y. Ma, H. Sun, M. Hu, Z. Feng, In-fiber quasi-Michelson interferometer with a core–cladding-mode fiber end-face mirror, Appl. Opt. 52 (2013) 1441–1447.
[14] Y. Wang, X. Tan, W. Jin, D. Ying, Y.L. Hoo, S. Liu, Temperature-controlled transformation in fiber types of fluid-filled photonic crystal fibers and applications, Opt. Lett. 35 (2010) 88–99.
[15] G. Yin, S. Lou, H. Zou, Refractive index sensor with asymmetrical fiber Mach–Zehnder interferometer based on concatenating single-mode abrupt taper and core-offset section, Opt. Laser Technol. 45 (2013) 294–300.
[16] Z.L. Ran, Y.J. Rao, W.J. Liu, X. Liao, K.S. Chiang, Laser-micromachined Fabry–Perot optical fiber tip sensor for high-resolution temperature-independent measurement of refractive index, Opt. Express 16 (2008) 2252–2263.
[17] Z. Tian, S.S. Yam, H.-P. Loock, Refractive index sensor based on an abrupt taper Michelson interferometer in a single-mode fiber, Opt. Lett. 33 (2008) 1105–1107.
[18] M.S. Meyer, G.L. Eesley, Optical fiber refractometer, Rev. Sci. Instrum. 58 (1987) 2047.
[19] C.B. Kim, C.B. Su, Measurement of the refractive index of liquids at 1.3 and 1.5 micron using a fibre optic Fresnel ratio meter, Meas. Sci. Technol. 15 (2004) 1683.
[20] H. Xue, H. Meng, W. Wang, R. Xiong, Q. Yao, B. Huang, Single-mode–multimode fiber structure based sensor for simultaneous measurement of refractive index and temperature, IEEE Sens. J. 13 (11) (2013) 4220–4223.
[21] S. Silva, O. Frazão, J. Santos, F. Malcata, A reflective optical fiber refractometer based on multimode interference, Sens. Actuators B: Chem. 161 (2012) 88–92.
[22] B.H. Lee, Y.H. Kim, K.S. Park, J.B. Eom, M.J. Kim, B.S. Rho, H.Y. Choi, Interferometric fiber optic sensors, Sensors 12 (2012) 2467–2486.
[23] J. Zhou, C. Liao, Y. Wang, G. Yin, X. Zhong, K. Yang, B. Sun, G. Wang, Z. Li, Simultaneous measurement of strain and temperature by employing fiber Mach–Zehnder interferometer, Opt. Express 22 (2014) 1680–1686.
[24] P. Lu, L. Men, K. Sooley, Q. Chen, Tapered fiber Mach–Zehnder interferometer for simultaneous measurement of refractive index and temperature, Appl. Phys. Lett. 94 (2009) 131110.
[25] Y. Kim, S.J. Park, S. Jeon, S. Ju, C. Park, W. Han, B.H. Lee, Thermo-optic coefficient measurement of liquids based on simultaneous temperature and refractive index sensing capability of a two-mode fiber interferometric probe, Opt. Express 20 (2012) 23744–23754.

Biographies

Jiangtao Zhou was born in Anhui province in China in 1990. He received his bachelor degree from Anhui University of Architecture in 2012. He is currently completing his master degree in the field of fiber optic sensors in Shenzhen University, China.

Yiping Wang is a Distinguished Professor and a Pearl River Scholar in the College of Optoelectronic Engineering, Shenzhen University, Shenzhen, China. He was born in Chongqing, China, in July 15, 1971. He received the B.S. degree in Precision Instrument Engineering from Xi'an Institute of Technology, Xi'an, China, in 1995, and the M.S. degree in Precision Instrument and Mechanism and the Ph.D. degree in Optical Engineering from Chongqing University, China, in 2000 and 2003, respectively, where he received the prestigious award of The National Excellent Doctoral Dissertations of China. In 2003, he joined the Department of Electronics Engineering, Shanghai Jiao Tong University, China, as a postdoctoral research fellow and an associate professor. In 2005, he joined the Department of Electrical Engineering, Hong Kong Polytechnic University, Hong Kong, as a postdoctoral research fellow and a research fellow. In 2007, he joined the Institute of Photonic Technology, Jena, Germany as a Humboldt research fellow. In 2009, he joined the Optoelectronics Research Centre, University of Southampton, U.K. as a Marie Curie Fellow. Since 2012, he has been with Shenzhen University as a Distinguished Professor and a Pearl River Scholar. His current research interests focus on optical fiber sensors, in-fiber gratings, photonic crystal fibers, and fluid-filling technologies. He has authored or coauthored 1 book, 9 patent applications, and more than 150 journal and conference papers with a SCI citation of more than 1200 times. Dr. Wang is a senior member of IEEE, the Optical Society of America, and the Chinese Optical Society.

Changrui Liao received the B.E. degree in optical information science and technology and the M.S. degree in physical electronics from Huazhong University of Science and Technology, China, in 2005 and 2007, and the Ph.D. degree from the Hong Kong Polytechnic University, Hong Kong, in 2012. Since 2012, he has been with the College of Optoelectronic Engineering, Shenzhen University as an assistant professor. His main research interests are femtosecond laser micromachining, optical fiber devices and sensors.

Bing Sun received bachelor degree and Ph.D. from Department of Science in Jiangsu University in 2008 and in 2013, respectively. He joined in Shenzhen University, China, as a postdoctoral fellow.

Jun He received bachelor degree and Ph.D. from Wuhan University and Chinese Academy of Sciences in 2008 and in 2013, respectively. He joined in Shenzhen University, China, as a postdoctoral fellow.

Guolu Yin received bachelor degree and Ph.D. from Department of Science in Beijing Jiaotong University in 2008 and in 2013, respectively. He joined in Shenzhen University, China, as a postdoctoral fellow.

Shen Liu was born in Henan Province, China in 1984, and received bachelor degree from Chongqing University of Posts and Telecommunication in 2013. He is currently completing her doctoral degree in the field of fiber optic sensors in Shenzhen University, China.

Zhengyong Li was born in Hubei Province, China in 1988. He received his bachelor degree from Huazhong University of Science and Technology Wenhua College in 2012. He is currently completing his master degree in the field of fiber optic sensors in Shenzhen University, China.

Guanjun Wang received bachelor degree and Ph.D. from Beijing University of Aeronautics and Astronautics in 2008 and in 2013, respectively. He joined in Shenzhen University, China, as a postdoctoral fellow.

Xiaoyong Zhong was born in Guangdong Province in China in 1988. He received bachelor degree in Guangdong University of Technology. He is currently completing his master degree in the field of fiber optic sensors in Shenzhen University, China.

Jing Zhao was born in Hubei Province, China in 1983, and received bachelor degree from University of Electronic Science and Technology of China in 2004. She is currently completing her doctoral degree in the field of fiber optic sensors in Shenzhen University, China.